Fluorescent diffuse photon density waves in homogeneous and heterogeneous turbid media: analytic solutions and applications

X. D. Li, M. A. O'Leary, D. A. Boas, B. Chance, and A. G. Yodh

We present analytic solutions for fluorescent diffuse photon density waves originating from fluorophores distributed in thick turbid media. Solutions are derived for a homogeneous turbid medium containing a uniform distribution of fluorophores and for a system that is homogeneous except for the presence of a single spherical inhomogeneity. Generally the inhomogeneity has fluorophore concentration, and lifetime and optical properties that differ from those of the background. The analytic solutions are verified by numerical calculations and are used to determine the fluorophore lifetime and concentration changes required for the accurate detection of inhomogeneities in biologically relevant systems. The relative sensitivities of absorption and fluorescence methods are compared.

1. Introduction

During the past few years many schemes have been developed to detect and image heterogeneities in biological tissues with diffusing near-IR light.[1] Most of these studies have centered on the detection of variations in the absorption and scattering coefficients in tissue and tissue phantoms. Recently, however, fluorescent contrast agents have also been considered as a means to enhance the specificity and sensitivity in tumor detection.[2–9] Fluorescent lifetime-based quantitation of different biological parameters such as tissue oxygenation pO_2,[10] pH value,[11] and intracellular calcium concentration $[Ca^{2+}]$ (Ref. 12) have been proposed by several investigators. Localized fluorophore concentration or lifetime variation may signal an increased number of small blood vessels associated with rapid tumor growth,[13] or the altered concentration of a fluorescence quencher that affects the fluorophore lifetime (e.g., the lowered concentration of oxygen from the high oxygen uptake in a rapidly growing tumor[14]). Thus functional imaging of the variations of fluorophore concentration and lifetime may provide useful clinical information.

Much effort has been devoted to formulating the forward problem of fluorescent light in turbid media. An integral form in the time domain has been given by Sevick-Muraca and co-workers[15,16] for the migration of fluorescent light in turbid media; these investigators have also numerically solved this integral equation in specific two-dimensional homogeneous and heterogeneous systems. A mathematical model for frequency-domain fluorescent-light propagation in semi-infinite homogeneous turbid media was obtained by Patterson and Pogue[3] using zero boundary conditions and assuming that the reduced scattering coefficients are the same for the excitation and the emission light. Finally a useful algorithm was developed by Wu *et al.*[17] to deconvolve fluorescent emission spectra from tissue reflectance measurements.

In this paper we derive more general analytic models to understand the response of fluorophores in homogeneous and heterogeneous turbid media. Our discussion is divided into three sections. In Subsection 2.A. we assume that the turbid medium is infinite and homogeneous and that the fluorophore concentration (number density) and lifetime are constant. In Subsection 2.B. we assume that the medium is infinite and heterogeneous, consisting of a spherical heterogeneity in an otherwise homogeneous turbid medium. The fluorophore concentra-

All authors are with the University of Pennsylvania, Philadelphia, Pennsylvania 19104. X. D. Li, M. A. O'Leary, and D. A. Boas are with the Department of Physics and Astronomy and the Department of Biochemistry and Biophysics. B. Chance is with the Department of Biochemistry and Biophysics. A. G. Yodh is with the Department of Physics and Astronomy.

Received 31 July 1995; revised manuscript received 27 February 1996.

0003-6935/96/193746-13$10.00/0

tion and lifetime are piecewise continuous in these models, simulating situations wherein fluorophores preferentially accumulate in tumors and may have environmentally sensitive lifetimes. In Subsection 2.C. we focus on analytic solutions for semi-infinite homogeneous systems. Numerical calculations where finite difference methods are used are performed in this case to verify the analytic solutions.

The analytic solutions reveal the explicit dependence of fluorescent diffusive waves on the fluorophore concentration, the lifetime, as well as the optical properties of the medium. In Section 3 these solutions are applied to expose signal-to-noise requirements for detecting heterogeneities that may arise in practical situations.

Although the analytic solutions derived in this paper are limited to some specific medium geometries (e.g., infinite and semi-infinite homogeneous media or heterogeneous media containing a single spherical object), the results presented here are useful because they are exact and enable rapid computations for signal-to-noise assessment over a broad range of experimental parameters. For example, the computation when analytic solutions are used for 100 arbitrary source–detector pairs in an infinite heterogeneous system containing a spherical object takes ~4 s of CPU time on a Sun Sparc10 workstation. Finite difference calculations, on the other hand, take ~20 min of CPU time for each source position.[18] Least-squared fitting procedures for determination of fluorophore concentration and lifetime based on these analytic solutions are thus possible within reasonable CPU times.

2. Theory

A. Photon Diffusion in Infinite Homogeneous Media

First we consider an infinite homogeneous turbid medium with a spatially uniform distribution of fluorophores. An intensity-modulated point light source with an optical wavelength that falls within the absorption band of the fluorophores creates an excitation diffuse photon density wave (DPDW) that excites the fluorophores. The fluorescent photons then add to create a fluorescent DPDW originating from the source fluorophore distribution. The fluorescent radiation is assumed to be well separated in energy from that of incident photons so that we can safely ignore the possibility of the excitation of fluorphores by the fluorescent reemission. We also assume that the excited fluorphores have a single lifetime.

1. Solution for a Point Source

In highly scattering media such as biological tissue, light propagation is well approximated by the photon diffusion equation that we adopt as a central assumption of our discussion,[19] i.e.,

$$\nabla^2\phi(\mathbf{r}, t) - \frac{v\mu_a}{D}\,\phi(\mathbf{r}, t) - \frac{1}{D}\,\frac{\partial\phi(\mathbf{r}, t)}{\partial t} = -\frac{v}{D}\,S(\mathbf{r}, t). \quad (1)$$

Here $\phi(\mathbf{r}, t)$ is the photon fluence rate [photons/(cm^2 s)], v is the speed of light in the turbid medium, μ_a is the absorption coefficient, $D = v/3\mu_s'$ is the photon diffusion coefficient where μ_s' is the reduced scattering coefficient, and $S(\mathbf{r}, t)$ is the source term that is the number of photons emitted at positon $\mathbf{r}$ and time t per unit volume per unit time.

For a point source at position $\mathbf{r}_s$ with an intensity modulation frequency f, we have $S(\mathbf{r}, t) = [M_{dc} + M_0 \exp(-i\omega t)]\delta(\mathbf{r} - \mathbf{r}_s)$, where M_{dc} and M_0 are the dc and ac parts of the source strength, respectively; ω is the angular modulation frequency, and $\omega = 2\pi f$. The resultant DPDW can be written as the sum of dc and ac parts, i.e., $\phi(\mathbf{r}, t) = \phi_{dc}(\mathbf{r}) + \phi_0(\mathbf{r})\exp(-i\omega t)$. In this paper we focus on the ac component. In an infinite homogeneous medium the ac solution to Eq. (1) is[20]

$$\phi_0(\mathbf{r}, \mathbf{r}_s) = \frac{vM_0}{D}\,\frac{\exp(ik|\mathbf{r} - \mathbf{r}_s|)}{4\pi|\mathbf{r} - \mathbf{r}_s|}. \quad (2)$$

Here the wave number k is complex, $k^2 = (-v\mu_a + i\omega)/D$. We see that the solution of the excitation DPDW in an infinite homogeneous system is a damped spherical wave.

In this paper we treat fluorophore and chromophore absorptions separately, but we assume that the change of scattering coefficient caused by the fluorophore is negligible for notational simplicity. (However, the fluorophore scattering effect is easily incorporated into the analytic solutions.) Absorption from tissue chromophores is characterized by absorption coefficient $\mu_a{}^c$. Absorption from exogenous fluorophores is characterized by an additional absorption coefficient σN_t, where N_t is the concentration of fluorophore and σ is the fluorophore absorption cross section (which is essentially the same as the fluorophore extinction coefficient, see Section 3). Thus in the presence of fluorophores the total absorption coefficient is the sum of these two coefficients, i.e., $\mu_a = \mu_a{}^c + \sigma N_t$.

2. Solutions for Fluorescent Diffusive Waves

Suppose that an intensity-modulated point source is at position $\mathbf{r}_s$ in a homogeneous system. The fluorophores in the medium are excited by the incident DPDW, ϕ_0, given in Eq. (2). Each excited fluorophore then acts as a secondary point source of fluorescent diffusive waves [Fig. 1(a)]. Treating fluorophores as two-level quantum systems and ignoring saturation effects, we find that the steady-state number density of excited fluorophores at position $\mathbf{r}$ is[21]

$$N_e(\mathbf{r}, \mathbf{r}_s) = \frac{\sigma N_t \eta}{\Gamma - i\omega}\,\phi_0(\mathbf{r}, \mathbf{r}_s), \quad (3)$$

where σ is the fluorophore absorption cross section at source wavelength λ_{ex}, N_t is the fluorophore concentration, $\Gamma = 1/\tau$ is the decay rate of an excited fluorophore, which is simply the reciprocal of fluorophore lifetime τ, and ϕ_0 is the incident photon fluence

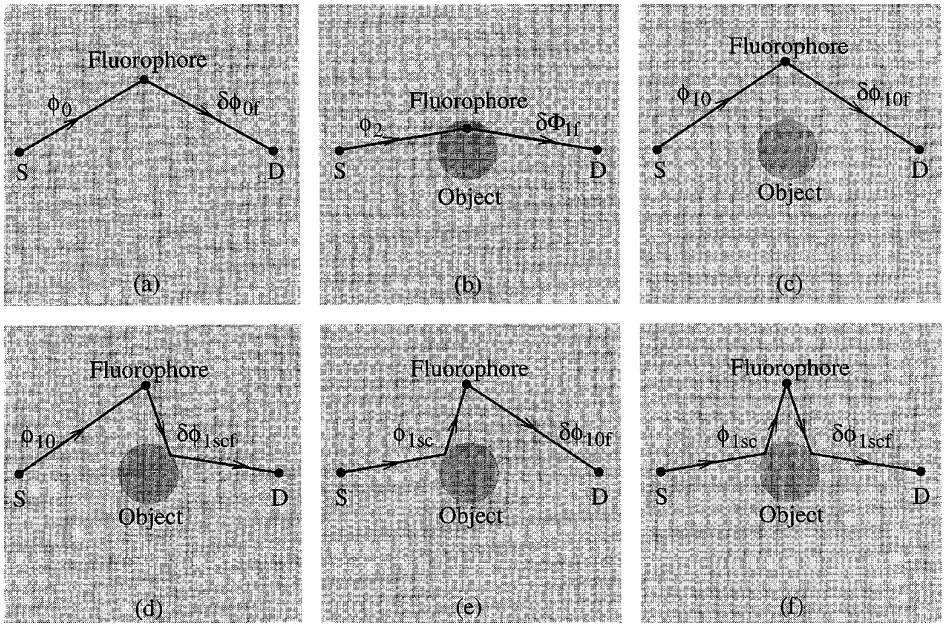

Fig. 1. Diagrammatic representation of fluorescent DPDW generated by fluorophores (a) in a homogeneous system and (b)–(f) in a heterogeneous system. (a) The fluorophore is excited by the excitation DPDW, and the reemission reaches the detector. (b) The fluorophore inside is excited, and the reemission reaches the detector. (c) The fluorophore outside is excited by the incident DPDW, and the reemission reaches the detector without being scattered by the sphere. (d) The fluorophore outside is excited by the incident DPDW, but the reemission is scattered by the sphere before reaching the detector. (e) The fluorophore outside is excited by the scattered DPDW, and the reemission reaches the detector without being scattered by the sphere. (f) The fluorophore outside is excited by the scattered DPDW, but the reemission is scattered by the sphere before reaching the detector.

rate [Eq. (2)]; η is the fluorescence quantum yield. For notational simplicity hereafter we assume excited fluorophores decay only through the radiation channel, i.e., $\eta = 100\%$. These excited fluorophores decay with a rate Γ, and thus the source term for fluorescent DPDW at position $\mathbf{r}$ is

$$S_f(\mathbf{r}, \mathbf{r}_s) = \Gamma N_e(\mathbf{r}, \mathbf{r}_s) = \frac{\sigma N_t}{1 - i\omega\tau}\,\phi_0(\mathbf{r}, \mathbf{r}_s). \tag{4}$$

Each fluorescence source generates a fluorescent DPDW that propagates to the detector at position $\mathbf{r}$. The detected fluorescent DPDW is found by integrating over all fluorescence sources, i.e.,

$$\phi_{0f}(\mathbf{r}, \mathbf{r}_s) = \int S_f(\mathbf{r}_1, \mathbf{r}_s)\,\frac{v}{D_f}\,\frac{\exp(ik_f|\mathbf{r} - \mathbf{r}_1|)}{4\pi|\mathbf{r} - \mathbf{r}_1|}\,d\mathbf{r}_1. \tag{5}$$

When the fluorophore distribution and lifetime are constant, one can solve the integral exactly by expanding the spherical waves in terms of spherical Bessel functions and spherical harmonics and then by using the appropriate orthogonality relations (see Appendix A). The analytic expression for the fluorescent DPDW in a homogeneous medium is

$$\phi_{0f}(\mathbf{r}, \mathbf{r}_s) = \frac{v^2 M_0}{D D_f}\,\frac{\sigma N_t}{1 - i\omega\tau}\,\frac{1}{k^2 - k_f^2} \times \left[\frac{\exp(ik|\mathbf{r} - \mathbf{r}_s|)}{4\pi|\mathbf{r} - \mathbf{r}_s|} - \frac{\exp(ik_f|\mathbf{r} - \mathbf{r}_s|)}{4\pi|\mathbf{r} - \mathbf{r}_s|}\right]. \tag{6}$$

Note that the fluorescent DPDW is a superimposition of two spherical waves with different DPDW wave numbers: One has the DPDW wave number k at the source wavelength λ_{ex}, and the other has the DPDW wave number k_f at the fluorescence wavelength λ_{fl}. The fluorescent DPDW is basically proportional to the fluorophore concentration (DPDW wave number k also depends on fluorophore concentration) and is explicitly related to the lifetime by a factor of $1/(1 - i\omega\tau)$. Note that a related result for a planar homogeneous medium has been derived in one dimension by Tromberg *et al.*[21]

B. Photon Diffusion in Infinite Heterogeneous Media Containing a Spherical Heterogeneity

A spherical object embedded in an otherwise homogeneous turbid medium may be of practical interest as a model for a tumor embedded in normal biological tissues. The analytic solution for fluorescent DPDW's in this case is useful in determining the fluorophore concentration contrast and lifetime changes necessary for detection of the object. Boas *et al.* have shown that the solution of DPDW's for a point source outside the sphere in a heterogeneous medium can be obtained by applying appropriate boundary conditions on the surface of the spherical object.[22] We treat the analogous problem for the fluorescent DPDW.

The problem is more complicated, however, because the fluorescent point sources are now distributed in space. In general, the incident light source

at λ_{ex} is outside the sphere whereas the fluorescent sources emitting at λ_{fl} can be inside and outside the sphere. We calculate the fluorescent DPDW generated by a point source inside and outside the sphere and then integrate the fluorescent DPDW over the corresponding source distribution to obtain the total fluorescent DPDW.

Before proceeding, we specify the following notation convention: All background quantities outside the sphere are denoted by subscript 1, e.g., ϕ_1, k_1, D_1, and all quantities inside the sphere are denoted by subscript 2, e.g., ϕ_2, k_2, D_2. Furthermore all fluorescence-related quantities are denoted by an extra subscript f, e.g., $\phi_{1f}, \phi_{2f}, k_{1f}, k_{2f}, D_{1f}, D_{2f}$. For simplicity we take the index of refraction $n_1 = n_2$. This enables us to ignore the optical reflection and refraction effects on the surface of the sphere. The speed of light is then the same everywhere, $v_1 = v_2 = v$. Differences in the indices of refraction can be accounted for by following the procedures set forth by Haskell *et al.*[23] and Aronson.[24]

For readers who are not interested in the details of the derivation, the main results are in Eq. (20) (the solution for the fluorescent DPDW generated by fluorophores inside a spherical object), Eq. (24) (the solution for the fluorescent DPDW generated by fluorophores outside the spherical object), and Eq. (25) [the sum of Eqs. (20) and (24), which is the solution for the fluorescent DPDW in an infinite heterogeneous turbid medium containing a spherical object]. Equations (26) and (27) are solutions for the fluorescent DPDW in a semi-infinite homogeneous system in which zero fluence rate boundary conditions and extrapolated zero fluence rate boundary conditions are used, respectively.

1. Solution for a Point Source

Consider an infinite system with a spherical heterogeneity of radius a at the origin and a point source at $\mathbf{r}_s$. In general we have two possible source configurations: a point source outside the sphere ($r_s > a$) and inside the sphere ($r_s < a$) as shown in Fig. 2.

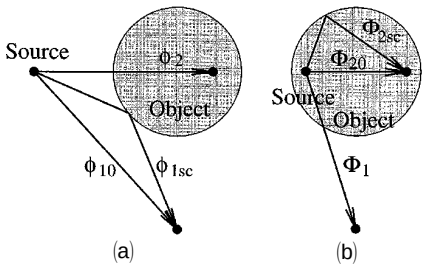

Fig. 2. Two source configurations in a heterogeneous medium containing a spherical object. (a) The source is outside the sphere, and the solution of DPDW outside the sphere [Eq. (7)] is the sum of the homogeneous incident part, ϕ_{10}, and the scattered part, ϕ_{1sc}. The solution inside the sphere is ϕ_2 as given by Eq. (8). (b) The source is inside the sphere, and the solution of DPDW outside the sphere is Φ_1 [Eq. (12)]. The solution inside the sphere is the sum of the homogeneous incident part, Φ_{20}, and the scattered part, Φ_{2sc}, as given by Eq. (13).

Physically we demand that the DPDW be finite at the origin ($r = 0$) and vanish at infinity ($r \to \infty$).

For a point source outside the sphere the resultant DPDW solutions outside and inside the sphere are

$$\phi_1(\mathbf{r}, \mathbf{r}_s) = \phi_{10}(\mathbf{r}, \mathbf{r}_s) + \phi_{1sc}(\mathbf{r}, \mathbf{r}_s) = \phi_{10}(\mathbf{r}, \mathbf{r}_s) + \sum_{lm} A_{lm}(\mathbf{r}_s) h_l^{(1)}(k_1 r) Y_{lm}(\Omega), \tag{7}$$

$$\phi_2(\mathbf{r}, \mathbf{r}_s) = \sum_{lm} B_{lm}(\mathbf{r}_s)\, j_l(k_2 r) Y_{lm}(\Omega), \tag{8}$$

where ϕ_{10} is the incident wave with background parameters [Eq. (2)], i.e.,

$$\phi_{10}(\mathbf{r}, \mathbf{r}_s) = \frac{v M_0}{D_1} \frac{\exp(ik_1|\mathbf{r} - \mathbf{r}_s|)}{4\pi|\mathbf{r} - \mathbf{r}_s|},$$

and ϕ_{1sc} is the scattered wave. The functions $h_l^{(1)}(k_1 r)$ and $j_l(k_2 r)$ are spherical Hankel functions of the first kind and spherical Bessel functions, respectively. The $Y_{lm}(\Omega)$ terms are spherical harmonics, and k_1 and k_2 are DPDW wave numbers. We found the coefficients A_{lm} and B_{lm} by requiring that the diffusive photon fluence rate and normal flux be continuous at the surface of the sphere, i.e.,

$$\phi_1(a, \mathbf{r}_s) = \phi_2(a, \mathbf{r}_s), \qquad D_1 \frac{\partial \phi_1(\mathbf{r}, \mathbf{r}_s)}{\partial r}_{|r=a} = D_2 \frac{\partial \phi_2(\mathbf{r}, \mathbf{r}_s)}{\partial r}_{|r=a}. \tag{9}$$

In this case we find that

$$A_{lm}(\mathbf{r}_s) = v \frac{-ik_1}{D_1} Q_l h_l^{(1)}(k_1 r_s) Y_{lm}^*(\Omega_s) M_0, \tag{10}$$

$$B_{lm}(\mathbf{r}_s) = v R_l h_l^{(1)}(k_1 r_s) Y_{lm}^*(\Omega_s) M_0, \tag{11}$$

where Q_l and R_l are constants that depend on the optical properties at λ_{ex}, modulation frequency, and the radius of the embedded spherical object (a). Their definitions are in Appendix B.

For the case of a point source inside the sphere at $\mathbf{r}_s (r_s < a)$, the solutions for the DPDW outside and inside the sphere are of the forms

$$\Phi_1(\mathbf{r}, \mathbf{r}_s) = \sum_{lm} C_{lm}(\mathbf{r}_s) h_l^{(1)}(k_1 r) Y_{lm}(\Omega), \tag{12}$$

$$\Phi_2(\mathbf{r}, \mathbf{r}_s) = \Phi_{20}(\mathbf{r}, \mathbf{r}_s) + \Phi_{2sc}(\mathbf{r}, \mathbf{r}_s) = \Phi_{20}(\mathbf{r}, \mathbf{r}_s) + \sum_{lm} D_{lm}(\mathbf{r}_s)\, j_l(k_2 r) Y_{lm}(\Omega). \tag{13}$$

Using the same boundary conditions for the fluence rate and normal flux on the surface of the sphere [Eq. (9)], we obtain

$$C_{lm}(\mathbf{r}_s) = v R_l\, j_l(k_2 r_s) Y_{lm}^*(\Omega_s) M_0, \tag{14}$$

$$D_{lm}(\mathbf{r}_s) = v \frac{-ik_2}{D_2} S_l\, j_l(k_2 r_s) Y_{lm}^*(\Omega_s) M_0, \tag{15}$$

where S_l is a constant that depends on the optical properties at λ_{ex}, modulation frequency, and the radius of the object. Its definition is given in Appendix B. R_l is the same as in Eq. (11).

2. Solutions for Fluorescent Diffusive Waves

We assume that the fluorophore distribution is piecewise uniform, i.e., the outside and inside fluorophore concentration N_1 and N_2 may be different but they are constant. We also assume that the excitation point source (at λ_{ex}) is outside the sphere at $\mathbf{r}_s (r_s > a)$. The source term for fluorophores outside and inside the sphere will be of the form

$$S_{1f}(\mathbf{r}_1, \mathbf{r}_s) = \frac{\sigma N_1}{1 - i\omega\tau_1}\,\phi_1(\mathbf{r}_1, \mathbf{r}_s), \tag{16}$$

$$S_{2f}(\mathbf{r}_2, \mathbf{r}_s) = \frac{\sigma N_2}{1 - i\omega\tau_2}\,\phi_2(\mathbf{r}_2, \mathbf{r}_s), \tag{17}$$

respectively, where $\phi_1(\mathbf{r}_1, \mathbf{r}_s)$ is given by Eq. (7) and $\phi_2(\mathbf{r}_2, \mathbf{r}_s)$ is given by Eq. (8).

The fluorescent DPDW measured at position $\mathbf{r}$ outside the sphere and generated by a fluorophore inside the sphere at position $\mathbf{r}_2$ with a source term $S_{2f}(\mathbf{r}_2, \mathbf{r}_s)$ is of the form of Eq. (12), i.e.,

$$\delta\Phi_{1f}(\mathbf{r}, \mathbf{r}_2, \mathbf{r}_s) = \sum_{lm} \delta C_{lm}{}^f(\mathbf{r}_2) h_l{}^{(1)}(k_{1f} r) Y_{lm}(\Omega), \tag{18}$$

where

$$\delta C_{lm}{}^f(\mathbf{r}_2) = v R_l{}^f j_l(k_{2f} r_2) Y_{lm}{}^*(\Omega_2) S_{2f}(\mathbf{r}_2, \mathbf{r}_s)\mathrm{d}\mathbf{r}_2, \tag{19}$$

and $\mathrm{d}\mathbf{r}_2$ is the volume element around position $\mathbf{r}_2$.

Figure 1(b) shows that the fluorophore inside the sphere at $\mathbf{r}_2$ is excited by incident DPDW $\phi_2(\mathbf{r}_2, \mathbf{r}_s)$ and the reemission propagates from $\mathbf{r}_2$ to a point at $\mathbf{r}$ outside the sphere. Integrating Eq. (18) over the entire space inside the sphere (i.e., over all possible $\mathbf{r}_2$), we derive the total contribution to the fluorescent DPDW from fluorophores inside the sphere, i.e.,

$$\begin{aligned}\Phi_{1f}(\mathbf{r}, \mathbf{r}_s) &= \int_{\text{Inside}} \delta\Phi_{1f}(\mathbf{r}, \mathbf{r}_2, \mathbf{r}_s) \\ &= M_0 v^2 \frac{\sigma N_2}{1 - i\omega\tau_2} \frac{a^2}{{k_2}^2 - {k_{2f}}^2} \\ &\quad \times \sum_{lm} \{[k_{2f} j_l(k_2 a) j_l{}'(k_{2f} a) - k_2 j_l{}'(k_2 a) \\ &\quad \times j_l(k_{2f} a)] R_l R_l{}^f h_l{}^{(1)}(k_{1f} r) h_l{}^{(1)}(k_1 r_s) \\ &\quad \times Y_{lm}(\Omega) Y_{lm}{}^*(\Omega_s)\},\end{aligned} \tag{20}$$

where constant $R_l{}^f$ has the same functional form as R_l except that it depends on the optical properties at λ_{fl} whereas R_l depends on the optical properties at λ_{ex}. It is defined in Appendix B.

Next we consider the fluorophores outside the sphere. The fluorescent DPDW measured at position $\mathbf{r}$ outside the sphere and generated by a fluorophore outside the sphere at $\mathbf{r}_1$ with a source term $S_{1f}(\mathbf{r}_1, \mathbf{r}_s)$ is of the form of Eq. (7), i.e.,

$$\begin{aligned}\delta\phi_{1f}(\mathbf{r}, \mathbf{r}_1, \mathbf{r}_s) &= \delta\phi_{10f}(\mathbf{r}, \mathbf{r}_1, \mathbf{r}_s) + \delta\phi_{1scf}(\mathbf{r}, \mathbf{r}_1, \mathbf{r}_s) \\ &= \delta\phi_{10f}(\mathbf{r}, \mathbf{r}_1, \mathbf{r}_s) + \sum_{lm} \delta A_{lm}{}^f(\mathbf{r}_1) \\ &\quad \times h_l{}^{(1)}(k_{1f} r) Y_{lm}(\Omega),\end{aligned} \tag{21}$$

where

$$\begin{aligned}\delta\phi_{10f}(\mathbf{r}, \mathbf{r}_1, \mathbf{r}_s) &= \phi_{10f}(\mathbf{r}, \mathbf{r}_1) S_{1f}(\mathbf{r}_1, \mathbf{r}_s)\mathrm{d}\mathbf{r}_1 \\ &= \frac{v}{D_{1f}} \frac{\exp(ik_{1f}|\mathbf{r} - \mathbf{r}_1|)}{4\pi|\mathbf{r} - \mathbf{r}_1|} \\ &\quad \times S_{1f}(\mathbf{r}_1, \mathbf{r}_s)\mathrm{d}\mathbf{r}_1,\end{aligned} \tag{22}$$

$$\begin{aligned}\delta A_{lm}{}^f(\mathbf{r}_1) &= \phi_{1scf}(\mathbf{r}, \mathbf{r}_1) S_{1f}(\mathbf{r}_1, \mathbf{r}_s)\mathrm{d}\mathbf{r}_1 \\ &= \left[v \frac{-ik_{1f}}{D_{1f}} Q_l{}^f h_l{}^{(1)}(k_{1f} r_1) Y_{lm}{}^*(\Omega_1)\right] \\ &\quad \times S_{1f}(\mathbf{r}_1, \mathbf{r}_s)\mathrm{d}\mathbf{r}_1,\end{aligned} \tag{23}$$

and $\mathrm{d}\mathbf{r}_1$ is the volume element around position $\mathbf{r}_1$.

The physical processes producing the fluorescent DPDW from fluorophores outside the sphere are shown in Figs. 1(c)–1(f). Integrating Eq. (21) over all space outside the sphere (i.e., over all possible $\mathbf{r}_1$), we obtain the contribution to the fluorescent DPDW from fluorophores outside the sphere, i.e.,

$$\begin{aligned}\phi_{1f}(\mathbf{r}, \mathbf{r}_s) &= \int_{\text{outside}} [\phi_{10f}(\mathbf{r}, \mathbf{r}_1) + \phi_{1scf}(\mathbf{r}, \mathbf{r}_1)] \frac{\sigma N_1}{1 - i\omega\tau_1} \\ &\quad \times [\phi_{10}(\mathbf{r}_1, \mathbf{r}_s) + \phi_{1sc}(\mathbf{r}_1, \mathbf{r}_s)]\mathrm{d}\mathbf{r}_1 \\ &= \frac{v^2 M_0}{D_1 D_{1f}} \frac{\sigma N_1}{1 - i\omega\tau_1} \frac{1}{{k_1}^2 - {k_{1f}}^2} \\ &\quad \times \left\{\left[\frac{\exp(ik_1|\mathbf{r} - \mathbf{r}_s|)}{4\pi|\mathbf{r} - \mathbf{r}_s|} - \frac{\exp(ik_{1f}|\mathbf{r} - \mathbf{r}_s|)}{4\pi|\mathbf{r} - \mathbf{r}_s|}\right]\right. \\ &\quad + \left[(ik_{1f}) \sum_{lm} Q_l{}^f h_l{}^{(1)}(k_{1f} r) h_l{}^{(1)}(k_{1f} r_s)\right. \\ &\quad + (-ik_1) \sum_{lm} Q_l h_l{}^{(1)}(k_1 r) h_l{}^{(1)}(k_1 r_s) \\ &\quad + (ik_1) \sum_{lm} Q_l E_l h_l{}^{(1)}(k_{1f} r) h_l{}^{(1)}(k_1 r_s) \\ &\quad \left.\left. + (-ik_1) \sum_{lm} F_l h_l{}^{(1)}(k_{1f} r) h_l{}^{(1)}(k_1 r_s)\right] \right. \\ &\quad \left. \times Y_{lm}{}^*(\Omega_s) Y_{lm}(\Omega)\right\},\end{aligned} \tag{24}$$

where the constant $Q_l{}^f$ has the same functional form as Q_l except that it depends on the optical properties at λ_{fl} whereas the constant Q_l depends on the optical properties at λ_{ex}. Constants E_l and F_l depend on the optical properties at λ_{ex} and the optical properties at

λ_{fl}. The definitions of these constants are given in Appendix B.

Note that the spherical region is devoid of outside fluorophores. The contribution from the outside fluorophores may be constructed by subtracting the solution for a sphere (containing the outside fluorophore) from the homogeneous solution—the first two terms in the braces in Eq. (24) [see also Eq. (6) and Fig. 1(a)]. All other terms are due to the presence of the spherical object and correspond to various combinations of the other three paths in Figs. 1(d)–1(f). Equation (24) is exact, but unfortunately after the algebraic simplifications some of the terms in Eq. (24) arise from combinations of different paths, and the physical origins of these terms are not always easily visualized as in Figs. 1(c)–1(f).

Finally the total fluorescent DPDW outside the sphere, $\phi_{\text{hetero}}^{fl}(\mathbf{r}, \mathbf{r}_s)$, generated by all the fluorophores inside and outside the sphere, is given by the sum of Eqs. (20) and (24):

$$\phi_{\text{hetero}}^{fl}(\mathbf{r}, \mathbf{r}_s) = \phi_{1f}(\mathbf{r}, \mathbf{r}_s) + \Phi_{1f}(\mathbf{r}, \mathbf{r}_s). \tag{25}$$

Note that in Eq. (25), $\Phi_{1f}(\mathbf{r}, \mathbf{r}_s)$ [see Eq. (20)] is the fluorescent DPDW generated by a fluorescing sphere with no background fluorophores whereas $\phi_{1f}(\mathbf{r}, \mathbf{r}_s)$ [see Eq. (24)] is the sum of the background term and the scattering terms. The total fluorescent DPDW is then the sum of $\Phi_{1f}(\mathbf{r}, \mathbf{r}_s)$ and $\phi_{1f}(\mathbf{r}, \mathbf{r}_s)$ [Eq. (25)].

In the forward calculation we take advantage of the symmetry of the system, e.g., if the light source is on the z axis, we have azimuthal asymmetry and we can remove the summation over m in Eqs. (20) and (24).

C. Semi-infinite Media and Numerical Verification of Analytic Solutions

In the above discussion we restricted our attention to infinite homogeneous and heterogeneous turbid media. The standard procedure for solving the diffusion equation for a semi-infinite homogeneous turbid medium is to approximate the exact zero partial current boundary condition with the extrapolated zero boundary condition.[23] For the excitation DPDW, we satisfy the extrapolated zero boundary condition by using the method of images, i.e., the DPDW in the medium is calculated from the superposition of the DPDW's generated by the real and the image sources. This situation becomes more complicated for the fluorescent DPDW. The fluorescent DPDW is generated by a uniform distribution of fluorophores (in half-space), and therefore we must consider a uniform distribution of image fluorophores to calculate the fluorescent DPDW. Suppose fluorophores distribute in the upper space, $z > 0$. The physical boundary of the fluorophores is the x–y plane at $z = 0$. For extrapolated zero boundary conditions, where the photon fluence rate is approximated to be zero in the x–y plane at $z = (2/3\mu_s')$, the resultant image fluorophores then distribute in the lower space, $z < -(4/3\mu_s')$. In this case a gap appears between the physical boundary of the fluorophores at the $z = 0$ plane and the corresponding image boundary of the image fluorophores at the $z = -(4/3\mu_s')$ plane. There are no fluorophores or image fluorophores inside this gap. Therefore the integral equation of the form of Eq. (5) cannot be evaluated analytically. However, using a less accurate zero boundary condition (where the photon fluence rate is zero at the physical boundary), we can calculate the integral analytically (see Appendix C), i.e.,

$$\phi_{0f}^{si-z.b.c.}(\mathbf{r}, \mathbf{r}_s) = \phi_{0f}(\mathbf{r}, \mathbf{r}_s) - \phi_{0f}(\mathbf{r}, \underline{\mathbf{r}_s^{zbc}}) \tag{26}$$

where $\mathbf{r}_s$ is the position of the real source and $\underline{\mathbf{r}_s^{zbc}}$ is the position of the image source with respect to the zero boundary; $\phi_{0f}(\mathbf{r}, \mathbf{r}_s)$ and $\phi_{0f}(\mathbf{r}, \underline{\mathbf{r}_s^{zbc}})$ are of the form of Eq. (6).

We have found that the extrapolated zero boundary condition can be implemented if we neglect the contribution of the gap. Neglecting the gap effect, we can take the solution in an infinite homogeneous system for a source at $\mathbf{r}_s$ and the solution for an image source at $\underline{\mathbf{r}_s^{ebc}}$, then superpose these two solutions. The resultant fluorescent DPDW ($\phi_{0f}^{si-e.b.c}$) for a semi-infinite homogeneous system with extrapolated zero boundary conditions has the same form as Eq. (26):

$$\phi_{0f}^{si-e.b.c.}(\mathbf{r}, \mathbf{r}_s) = \phi_{0f}(\mathbf{r}, \mathbf{r}_s) - \phi_{0f}(\mathbf{r}, \underline{\mathbf{r}_s^{ebc}}), \tag{27}$$

where $\mathbf{r}_s$ is the position of the real source and the $\underline{\mathbf{r}_s^{ebc}}$ is the position of the image source with respect to the extrapolated zero boundary; $\phi_{0f}(\mathbf{r}, \mathbf{r}_s)$ and $\phi_{0f}(\mathbf{r}, \underline{\mathbf{r}_s^{ebc}})$ are of the form of Eq. (6).

This is an extension of the result that we obtained in Appendix C using zero boundary conditions to approximate the exact zero partial current boundary conditions. Equation (27) turns out to be a very good approximation. Numerical calculations of fluorescent DPDW's at different modulation frequencies (f) where a finite difference algorithhm is used[25] have been performed to verify Eq. (27) for two fluorophore lifetimes (1 and 2 ns). The basic procedure is to solve the diffusion equation [Eq. (1)] for the fluorescence DPDW in the time domain by using the exact zero partial current boundary condition[23] and then Fourier transform the data into the frequency domain. In the calculations the fluorophore concentration is assumed to be $N_t = 0.1$ μM. The source and the detector are placed on the surface of the medium with a 2-cm separation, and the optical properties (μ_{a1}, μ_{s1}', μ_{a1f}, μ_{s1f}', σ) are given in Table 1. Results are shown in Fig. 3 in which we plot the theoretical amplitude and phase calculated by using Eq. (27) and the amplitude and phase calculated by using the finite difference method. The ratio of the normalized amplitude and the residual of the phase are also shown in Fig. 3. We find that the analytic solution of the fluorescent DPDW for a semi-infinite homogeneous system using an extrapolated zero boundary condition [Eq. (27)] agrees with the finite

Table 1. Chromophore Optical Properties at λ_{ex} and λ_{fl} and Other Parameters[a]

$\mu_{a1}{}^{c}$	$\mu_{s1}{}'$	$\mu_{a2}{}^{c}$	$\mu_{s2}{}'$	$\mu_{a1f}{}^{c}$	$\mu_{s1f}{}'$	$\mu_{a2f}{}^{c}$	$\mu_{s2f}{}'$	σ ($cm^{-1}\,M^{-1}$)	f (MHz)	r_{sd} (cm)
0.02	8.0	0.04	10.0	0.025	8.0	0.05	10.0	6×10^4	200	6

[a]The optical properties are in units of cm^{-1}; r_{sd} is the source–detector separation.

difference results with an accuracy of better than 3% in amplitude and 1.2° in phase up to an 800-MHz modulation frequency. Using a zero boundary condition [Eq. (26)] for the same system, we find that a little larger discrepancy, in particular, ~4% in amplitude and 1.5° in phase, was observed. These discrepancies are mainly due to a numerical computation error. If we reduce the grid size from $1/\mu_s'$ to $1/(2\mu_s')$ in the finite difference calculations, we find that these discrepancies decrease, e.g., less than 1.2% in amplitude and less than 1° in phase for a semi-infinite homogeneous system using an extrapolated zero boundary condition [Eq. (27)]. The tradeoff of using a smaller grid size is a much longer computation time. As we mentioned in Section 1, the analytic calculation is much faster than the numerical calculation. For $\tau = 1$ ns in the above calculations, the analytic method takes ~0.1 s of CPU time (modulation frequency f varies from 0 to 1 GHz with a step of 50 MHz), but the finite difference method takes ~25 min. For a longer lifetime (e.g., $\tau = 2$ ns) the numerical method requires a longer CPU time (e.g., ~1 h) whereas the analytic method still takes ~0.1 s of CPU time.

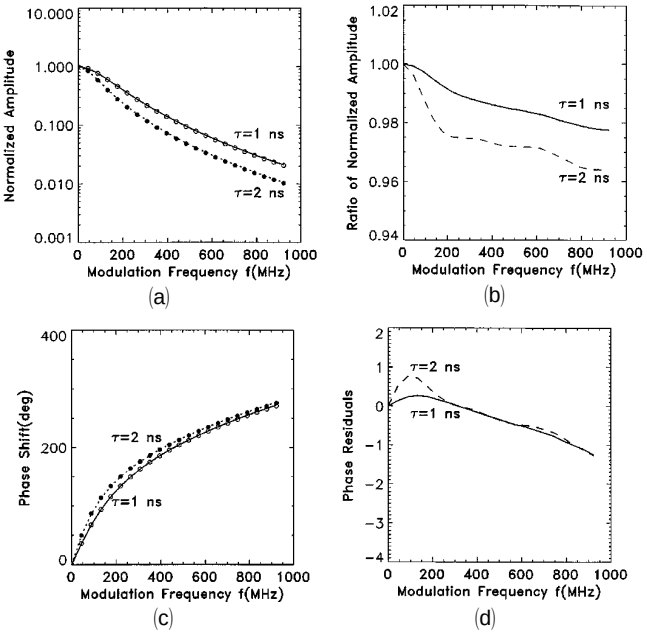

Fig. 3. Comparison of the analytic solution [Eq. (27)] and the finite difference method for a semi-infinite homogeneous system. The source and detector are placed on the surface of the medium 2 cm apart. (a) Amplitude normalized by the dc amplitude ($f = 0$ MHz). The solid curve and the open circles represent normalized amplitudes for $\tau = 1$ ns as calculated by the analytic solutions and the finite difference method, respectively. The dashed curve and filled circles represent normalized amplitudes for $\tau = 2$ ns as calculated by the analytic solutions and the finite difference method, respectively. (b) Ratio of the normalized amplitude calculated by the finite difference methods and the normalized amplitude calculated by analytic solutions (solid curve, $\tau = 1$ ns; dashed curve, $\tau = 2$ ns). (c) Phase with respect to the dc phase (which is zero). The solid curve and the open circles represent phases for $\tau = 1$ ns calculated by analytic solutions and the finite difference method, respectively. The dashed curve and filled circles represent phases for $\tau = 2$ ns calculated by analytic solutions and the finite difference method, respectively. (d) Phase residues that are the difference between the phase calculated by the finite difference method and the phase calculated by analytic solutions (solid curve, $\tau = 1$ ns; dashed curve, $\tau = 2$ ns).

As for the semi-infinite heterogeneous system, the situation will be much more complicated because we must consider not only the image source but also the image object as well as the image fluorophores. Nevertheless in analogy with semi-infinite homogeneous media observations, one can be encouraged to employ the same basic procedure as used in the above analysis. Finite difference calculations of the fluorescent DPDW in a semi-infinite heterogeneous turbid media containing a spherical object have been performed for different fluorophore concentration and lifetime contrasts. We found good agreement between the finite difference results and the results calculated by the analytic solutions, following the same basic procedure as for the semi-infinite homogeneous media. Consider a semi-infinite system with a 0.6-cm radius object 3 cm deep in the medium. The source and the detector are placed on the surface of the medium and separated by 2 cm. An accuracy of better than 1.8% in amplitude and 1.2° in phase to an 800-MHz modulation frequency is obtained when the optical properties given in Table 1 are used.

3. Applications

Analytic solutions reveal the manner in which fluorescent DPDW's are related to the spatial distribution of fluorophore lifetimes and concentrations. We now apply these solutions to several problems of practical importance. First, we discuss the fitting procedure for determination of the fluorophore lifetime and concentration in homogeneous media. Next we calculate the fluorophore concentration contrast and the lifetime variation necessary to detect an object embedded in an otherwise homogeneous medium. Finally we compare the sensitivities of fluorophores as absorption contrast and fluorescent contrast for the detection of spherical objects in turbid media.

In general we take the fluorophore absorption cross section (σ) to be $\sim 10^{-16}$ cm^2 for near-IR excitation light.[26] The absorption cross section is related to the extinction coefficient by Avogadro's constant,

i.e., $\varepsilon(\mathrm{cm}^{-1}\,\mathrm{M}^{-1}) = \sigma(\mathrm{cm}^2) \times N^{\mathrm{Avog}} \times 10^{-3}$. In terms of the extinction coefficient the above absorption cross section is $6.0 \times 10^4\ \mathrm{cm}^{-1}\,\mathrm{M}^{-1}$. Unless stated otherwise, we assume this value for the fluorophore absorption cross section. In the following simulations the fluorophore concentration in homogeneous media is assumed to be $N_t = 0.1$ μM. The background concentration (outside the sphere) in the heterogeneous media is also assumed to be $N_1 = 0.1$ μM. Different concentrations inside the sphere are considered. We choose the concentration to be in the micromolar regime for three reasons: (1) Such concentrations are realistically expected for experiments *in vivo*.[7] (2) Fluorescence saturation effects can be ignored. (3) The fluorophore absorption is comparable with the chromophore absorption when the fluorophore is used as an absorption contrast.

A. Fitting Procedure for Determination of Fluorophore Concentration and Lifetime in Homogeneous Systems

Fluorophore lifetime is a good indicator of the fluorophore tissue environment (e.g., the pH or pO_2 value). One way to determine the fluorophore lifetime in homogeneous media is to measure the phase and/or the amplitude of the fluorescent DPDW at different modulation frequencies. The predicted dependence of the amplitude and phase of fluorescent DPDW on the modulation frequency (f) for three different lifetimes is illustrated in Fig. 4. The differences in the curves indicate the sensitivity to fluorophore lifetime τ. The optical properties (μ_{a1}, μ_{s1}', μ_{a1f}, μ_{s1f}', σ), the source–detector separation (r_{sd}), and the modulation frequence (f) used in the simulation are given in Table 1. With experimental data, we can obtain accurate lifetimes and concentration by fitting the amplitude and phase curves of the fluorescent DPDW with the analytic solution [Eq. (6)] at multiple modulation frequencies. In such cases the tissue optical properties at λ_{ex} and λ_{fl} should be measured before adding fluorophores into the system to reduce the number of free parameters in the fit.

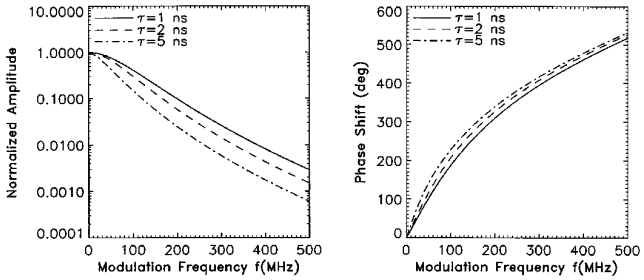

Fig. 4. Fluorescent DPDW [Eq. (6)] versus the modulation frequency (f) in an infinite homogeneous turbid medium for three different lifetimes (τ = 1, 2, and 5 ns): (a) normalized amplitude, (b) phase shift. The amplitude is normalized by the amplitude at zero modulation frequency ($f = 0$) for each curve at the corresponding fluorophore lifetime, and the phase is phase shifted with respect to the phase at the zero modulation frequency. Solid curves, τ = 1 ns; dashed curves, τ = 2 ns; dash–dotted curve, τ = 5 ns. Source–detector separation r_{sd}, 6 cm. The optical properties ($\mu_{a1}{}^c$, μ_{s1}' for incident DPDW at λ_{ex} and $\mu_{a1f}{}^c$, μ_{s1f}' for fluorescent DPDW at λ_{fl}) are given in Table 1.

Using the same optical parameters and source–detector separation (6 cm) as in Fig. 4, we calculate the amplitude and phase of the fluorescent DPDW for $N_t = 0.1$ μM and $\tau = 1.0$ ns at multiple modulation frequencies (0–500 MHz in 50-MHz steps). We then add 2% random noise to the amplitude and 1° random noise to the phase. The noisy data are fitted with the analytic solution [Eq. (6)] where we assume that all the parameters are known except the fluorophore concentration and lifetime. For six independent least-square fittings, we obtain the fluorophore concentration, $N_t{}^{\mathrm{fit}} = (0.1002 \pm 0.0007)$ μM and lifetime $\tau^{\mathrm{fit}} = (1.003 \pm 0.007)$ ns. For the data with 5% amplitude noise and 5° phase noise, the fitted results are still very close to real values, e.g., $N_t{}^{\mathrm{fit}} = (0.1003 \pm 0.0017)$ μM and $\tau^{\mathrm{fit}} = (1.005 \pm 0.016)$ ns.

Another method suggested by Sevick-Muraca and co-workers for lifetime measurements in homogeneous turbid media is to introduce a reference fluorophore with a known lifetime. They pointed out that the unknown fluorophore lifetime can then be obtained from the relative phase shift between the fluorescent DPDW generated from fluorophores with unknown lifetime and the fluorescent DPDW generated from reference fluorophores with a known lifetime.[16] This relationship is easily verified for homogeneous media where the analytic solution is used. In Eq. (6) we see that the phase of the fluorescent DPDW caused by the fluorophore lifetime is $\tan^{-1}(\omega\tau)$. If we assume that the optical properties are the same for the fluorophore with lifetime τ_2 (unknown) and the fluorophore with lifetime τ_1 (known), we obtain the relative phase shift θ_{21}:

$$\theta_{21} = \tan^{-1}\left[\frac{\omega(\tau_2 - \tau_1)}{1 + \omega^2\tau_1\tau_2}\right] = \tan^{-1}(\omega\tau_2) - \tan^{-1}(\omega\tau_1), \tag{28}$$

which is in agreement with the result in Ref. 16. For a homogeneous system, Eq. (28) provides a simple relationship between the phases of the fluorescent DPDW's generated by two kinds of fluorophore with different lifetimes, and it is valid as long as the the optical properties of the medium are the same for the two fluorophores.

B. Required Contrast of Fluorophore Concentration and Lifetime for Detection and Characterization of a Spherical Heterogeneity

The variations in fluorophore distribution and lifetime in normal and malignant tissues may give enhanced sensitivity and specificity for tumor detection. Using Eq. (25), we calculate the amplitude and the phase of the fluorescent DPDW for a heterogeneous system containing a spherical object. The required phase precision to detect such an object with fluorescent DPDW's is determined from the

position-dependent phase difference between the fluorescent DPDW in the heterogeneous medium and the fluorescent DPDW in the homogeneous medium with the same background optical properties. The required amplitude precision is found from a similar position-dependent normalized amplitude $|\phi_{\text{hetero}}{}^{fl}/\phi_{0f}|$ [see Eqs. (6) and (25)]. Figure 5 shows contour plots of the spatially dependent normalized amplitude and the phase shift for an object of 0.6-cm radius at the origin in a medium with the optical properties given in Table 1. The source is located 3 cm from the object. A detector would scan in the plane that contains the source and the center of the object. In the calculation the lifetimes of the fluorophore outside and inside the sphere are assumed to be equal, i.e., $\tau_1 = \tau_2 = 1$ ns, and the concentration contrast N_2/N_1 is assumed to be 5. We see that differential amplitude and phase signals from an object of 0.6-cm radius (within ~4 cm of the object) is detectable with the 0.1° phase and 0.1% amplitude measurement precisions achievable with current technologies.

Some fluorophores may be tumor specific and the fluorophore concentration inside the tumor may be higher than in the surrounding normal tissues. Normalized amplitudes and phase shifts of the fluorescent DPDW versus fluorophore contrast N_2/N_1 are calculated for objects of three different sizes by using the parameters given in Table 1. The objects are always centered between the source and the detector. Results are shown in Fig. 6. We find that, if our system is limited by 0.1% amplitude noise and 0.1° phase noise, a contrast, $N_2/N_1 \sim 5$, gives us differentiable fluorescence signals for an object of 0.5-cm radius.

The fluorophore lifetime can be altered by the environment.[27] This is another possible indicator for tumor detection.[28] If the fluorophore lifetime inside the object (τ_2) increases, the fluorescent DPDW amplitude decreases and the phase shift resulting from τ_2 saturates for $\omega\tau_2 \gg 1$. If, on the other hand, τ_2 decreases and $\omega\tau_2 \ll 1$, the amplitude and the phase are no longer sensitive to τ_2. We see, however, that a regime exists wherein the change of τ_2 gives enhanced sensitivity to the detection of the heterogeneity. In Fig. 7 we show the lifetime ratio (τ_2/τ_1) dependence of fluorescent DPDW's for three different size objects, again centered between the source and the detector, using the parameters given in Table 1. We assume the fluorophore concentration contrast, $N_2/N_1 = 5$, in the calculation and find that when $0.2 \le \tau_2/\tau_1 \le 1.8$ the amplitude and phase provide signals above the defined noise level for the detection of an object of 0.5-cm radius.

If we assume that all the parameters are known except the fluorophore concentration and lifetime inside the object, e.g., N_2 and τ_2, we can use the data at multiple modulation frequencies (0–500 MHz in 50-MHz steps, added with 2% amplitude noise and 1° phase noise) to fit for the concentration and the lifetime. In this case we find that N_2 and τ_2 obtained from the fitting procedure are close to their real values, i.e., $N_2{}^{\text{fit}} = (0.508 \pm 0.015)$ μM and $\tau_2{}^{\text{fit}} = (1.530 \pm 0.060)$ ns where the real concentration and lifetime are $N_2 = 0.5$ μM and $\tau_2 = 1.5$ ns. The errors in $N_2{}^{\text{fit}}$ and $\tau_f{}^{\text{fit}}$ are the standard errors for six independent fittings. In the calculation a spherical

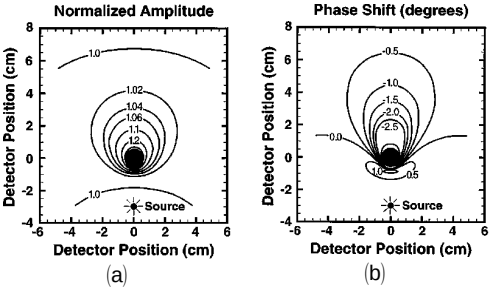

Fig. 5. Contour plots in a plane that contains the source and the object illustrating the required phase and amplitude precision to detect and localize an object of 0.6-cm radius. (a) Contours of the normalized amplitude. (b) Contours of the phase shift. The optical properties are given in Table 1. Fluorophore lifetimes inside and outside the sphere are assumed to be equal ($\tau_1 = \tau_2 = 1$ ns), and the fluorophore concentration contrast is assumed to be 5.

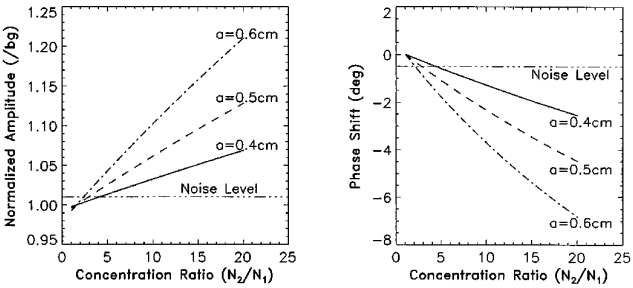

Fig. 6. Fluorescent DPDW versus fluorophore concentration contrast in a heterogeneous system. The source and the detector are separated by 6 cm, and the object is halfway between them. In the simulation the lifetimes inside and outside the sphere are assumed to be equal ($\tau_1 = \tau_2 = 1$ ns). The system parameters are given in Table 1. The amplitude is normalized by the amplitude in a homogeneous system, and the phase shift is with respect to the phase in a homogeneous system.

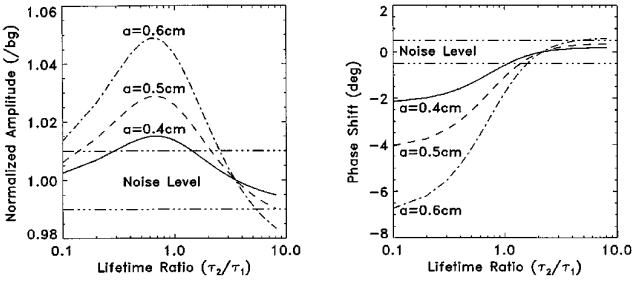

Fig. 7. Fluorescent DPDW versus a fluorophore lifetime change in a heterogeneous system. An object is centered between the source and the detector for a source–detector separation, $r_{sd} = 6$ cm. We assume that the lifetime outside the sphere is $\tau_1 = 1$ ns and that the fluorophore concentration contrast, N_2/N_1, is 5. The parameters are given in Table 1. The amplitude is normalized by the amplitude in a homogeneous system, and the phase shift is with respect to the phase in a homogeneous system. The nosie level is indicated by the dashed–dotted curves.

object of 0.6-cm radius is centered between the source and the detector, and the source–detector separation is 6 cm. Background fluorophore concentration and lifetime are assumed to be $N_1 = 0.1$ μM and $\tau_1 = 1.0$ ns, respectively. The optical properties are given in Table 1. Note that in practice the fitting procedure to obtain the fluorophore concentration and lifetime inside the object is more difficult, because there are more unknown parameters such as the optical properties inside the object and the size and the position of the object. Thus the fitting procedure above for heterogeneous media provides best-case estimates.

C. Comparison of Absorption and Fluorescence Sensitivities of Fluorophores in Heterogeneous Media

Fluorophores increase the local absorption coefficient by an amount σN_t as discussed in Section 2. In a turbid system, and in the presence of a spherical object, the excitation DPDW amplitude [Eqs. (7) and (8)] decreases exponentially as the absorption coefficient of the object increases. An increase in fluorophore absorption cross section (σ) will thus enhance the total absorption coefficient. As for the fluorescent DPDW, an increase in σ introduces two competing effects: The amplitude of the excitation DPDW that is related to the fluorescence source terms [Eq. (16) and (17)] decreases exponentially as σ increases, but the fluorescent DPDW amplitude increases linearly as σ increases. The phase of the excitation DPDW and fluorescent DPDW always increases when σ increases. Our calculations of the normalized amplitude and phase shift of the excitation and fluorescent DPDW's versus fluorophore absorption cross section are shown in Fig. 8. Here we use the parameters (except the absorption cross section σ) given in Table 1. The fluorophore concentration contrast is $N_1/N_2 = 5$, and the object radius is 0.5 cm. Fluorophore lifetimes inside and outside of the object are taken to be equal (1 ns). The normalized amplitude for the excitation DPDW is $|\phi_1/\phi_{10}|$, and the phase shift is the phase difference between these two DPDW's [see Eqs. (7) and (6)]. The normalized amplitude and phase shift for the fluorescent DPDW are the same as in Subsection 3.B. We find that for smaller fluorophore absorption cross sections, e.g., $\sigma \le 6 \times 10^4$ cm^{-1}M^{-1}, the fluorescent DPDW gives a better sensitivity, whereas the excitation DPDW gives a better sensitivity for bigger fluorophore absorption cross sections, e.g., $\sigma \ge 6 \times 10^4$ cm^{-1}M^{-1}.

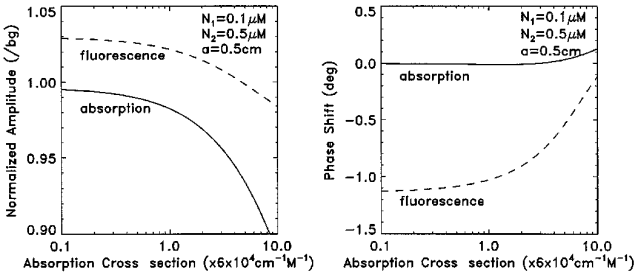

Fig. 8. Comparison of absorption and fluorescence of fluorophores in a heterogeneous medium. An object is centered between the source and the detector for $r_{sd} = 6$ cm. We assume that the lifetimes outside and inside the sphere are equal ($\tau_1 = \tau_2 = 1$ ns) and that the fluorophore concentration contrast, N_2/N_1, is 5. The parameters are given in Table 1. The amplitude is normalized by the corresponding amplitude in a homogeneous system, and the phase shift is with respect to the corresponding phase in a homogeneous system.

In the discussion above, we assumed that the noise levels for the excitation DPDW and fluorescent DPDW are comparable (e.g., 1% amplitude noise and 0.5° phase noise) and that the noise is mainly due to such factors as the source and detector positional errors rather than the shot noise. For a 0.1-mW light source the excitation DPDW fluence rate is $\sim 10^{11}$ photons/(cm^2 s) at the detector for a 6-cm source–detector separation in a homogeneous medium or in a heterogeneous medium with an object of ~0.5-cm radius centered between the source and the detector. The fluorescent DPDW fluence rate in this case is lower than the excitation DPDW fluence rate by ~2–3 orders of magnitude when reasonable concentrations and fluorophore absorption cross sections are used, e..g, $\sigma N_t \sim \mu_a{}^c$. Even with the loss of 2 orders of magnitude of photon-fluence rate resulting from the detection area and the optical coupling, we find that our detection of heterogeneities is still not shot noise limited in either case.

4. Conclusions

We have presented analytic solutions for fluorescent diffuse photon density waves in homogeneous and heterogeneous turbid media. Using these results and considering a simplified heterogeneous system containing a single spherical object, we conclude that approximately fivefold fluorophore concentration contrast and lifetime variation of a factor of 0.2–1.8 provide an observable differential signal to detect an object of 0.5-cm radius centered between the source and the detector with $r_{sd} = 6$ cm. This frequency-domain analysis can easily be applied to time-domain experiments by Fourier transformation of the time-domain data. Tomographic image reconstruction techniques can also be used for fluorescence lifetime imaging in turbid media.[29]

Appendix A. Basic Relations Used in the Derivation of Analytic Solutions

The Green's function can be expanded in terms of spherical Bessel functions and spherical harmonics:

$$G(\mathbf{r}_1, \mathbf{r}_2, k) = \frac{\exp(ik|\mathbf{r}_1 - \mathbf{r}_2|)}{4\pi|\mathbf{r}_1 - \mathbf{r}_2|} = ik \sum_{lm} j_l(kr_<) \times h_l^{(1)}(kr_>) Y_{lm}^*(\Omega_1) Y_{lm}(\Omega_2), \quad \text{(A1)}$$

where $r_< = \min(r_1, r_2)$, $r_> = \max(r_1, r_2)$. The orthogo-

nality relation of spherical harmonics is

$$\int_{4\pi} Y_{lm}(\Omega) Y_{l'm'}{}^{*}(\Omega) \mathrm{d}\Omega = \delta_{l,l'} \delta_{m,m'}. \tag{A2}$$

The following integral of the product of two Bessel functions is used to perform the radial integration:

$$\int f_l(k_1 r) g_l(k_2 r) r^2 \mathrm{d}r = \frac{r^2}{{k_1}^2 - {k_2}^2} [k_2 f_l(k_1 r) g_l{}'(k_2 r) - k_1 f_l{}'(k_1 r) g_l(k_2 r)], \tag{A3}$$

where $f_l(x)$ and $g_l(y)$ are any spherical Bessel functions of order l and $f_l{}'(x)$ and $g_l{}'(y)$ are the derivatives of the spherical Bessel function with respect to the x and y argument, respectively.

Appendix B. Definitions of Constants Used in the Analytic Solutions

In solving the heterogeneous problem, we obtain several constants of similar functional forms by matching the boundary condition [Eq. (9)]. They are defined as

$$Q_l = \frac{D_2 k_2 j_l(k_1 a) j_l{}'(k_2 a) - D_1 k_1 j_l{}'(k_1 a) j_l(k_2 a)}{D_2 k_2 h_l{}^{(1)}(k_1 a) j_l{}'(k_2 a) - D_1 k_1 h_l{}'^{(1)}(k_1 a) j_l(k_2 a)}, \tag{B1}$$

$$Q_l{}^f = \frac{D_{2f} k_{2f} j_l(k_{1f} a) j_l{}'(k_{2f} a) - D_{1f} k_{1f} j_l{}'(k_{1f} a) j_l(k_{2f} a)}{D_{2f} k_{2f} h_l{}^{(1)}(k_{1f} a) j_l{}'(k_{2f} a) - D_{1f} k_{1f} h_l{}'^{(1)}(k_{1f} a) j_l(k_{2\,f} a)}, \tag{B2}$$

$$R_l = \frac{1}{a^2 [D_2 k_2 h_l{}^{(1)}(k_1 a) j_l{}'(k_2 a) - D_1 k_1 h_l{}'^{(1)}(k_1 a) j_l(k_2 a)]}, \tag{B3}$$

$$R_l{}^f = \frac{1}{a^2 [D_{2f} k_{2f} h_l{}^{(1)}(k_{1f} a) j_l{}'(k_{2f} a) - D_{1f} k_{1f} h_l{}'^{(1)}(k_{1f} a) j_l(k_{2f} a)]}, \tag{B4}$$

$$S_l = \frac{D_2 k_2 h_l{}^{(1)}(k_1 a) h_l{}'^{(1)}(k_2 a) - D_1 k_1 h_l{}'^{(1)}(k_1 a) h_l{}^{(1)}(k_2 a)}{D_2 k_2 h_l{}^{(1)}(k_1 a) j_l{}'(k_2 a) - D_1 k_1 h_l{}'^{(1)}(k_1 a) j_l(k_2 a)}, \tag{B5}$$

$$E_l = \frac{D_{2f} k_{2f} h_l{}^{(1)}(k_1 a) j_l{}'(k_{2f} a) - D_{1f} k_1 h_l{}'^{(1)}(k_1 a) j_l(k_{2f} a)}{D_{2f} k_{2f} h_l{}^{(1)}(k_{1f} a) j_l{}'(k_{2f} a) - D_{1f} k_{1f} h_l{}'^{(1)}(k_{1f} a) j_l(k_{2f} a)}, \tag{B6}$$

$$F_l = \frac{D_{2f} k_{2f} j_l(k_1 a) j_l{}'(k_{2f} a) - D_{1f} k_1 j_l{}'(k_1 a) j_l(k_{2f} a)}{D_{2f} k_{2f} h_l{}^{(1)}(k_{1f} a) j_l{}'(k_{2f} a) - D_{1f} k_{1f} h_l{}'^{(1)}(k_{1f} a) j_l(k_{2f} a)}, \tag{B7}$$

where superscript or subscript f corresponds to the optical properties at fluorescent wavelength λ_{fl}.

Appendix C. Analytic Solution in a Semi-infinite Homogeneous System

Consider a semi-infinite homogeneous system with a physical boundary at $z = 0$ and a uniform fluorophore distribution in $z > 0$ half-space. For the zero boundary condition, if the real source is at position $\mathbf{r}_s = (x_s, y_s, z_s)$, the image source will be at position $\underline{\mathbf{r}}_s = (x_s, y_s, -z_s)$. The excitation DPDW is thus

$$\phi_0{}^{si}(\mathbf{r}', \mathbf{r}_s) = \frac{v M_0}{D} \left[\frac{\exp(ik|\mathbf{r}' - \mathbf{r}_s|)}{4\pi|\mathbf{r}' - \mathbf{r}_s|} - \frac{\exp(ik|\mathbf{r}' - \underline{\mathbf{r}}_s|)}{4\pi|\mathbf{r}' - \underline{\mathbf{r}}_s|} \right]. \tag{C1}$$

As we have seen in Section 2 [Eq. (4)], the source term for the fluorescent DPDW from the real fluorophore at position $\underline{\mathbf{r}}'$ in $z > 0$ half-space is

$$S_f{}^{\mathrm{real}}(\mathbf{r}', \mathbf{r}_s) = \frac{\sigma N_t}{1 - i\omega\tau} \phi_0{}^{si}(\mathbf{r}', \mathbf{r}_s). \tag{C2}$$

Therefore the source term from the corresponding image fluorophore at position $\mathbf{r}'$ has the same source strength but with a negative sign:

$$S_f{}^{\mathrm{img}}(\underline{\mathbf{r}}', \mathbf{r}_s) = -S_f{}^{\mathrm{real}}(\mathbf{r}', \mathbf{r}_s) = -\frac{\sigma N_t}{1 - i\omega\tau} \phi_0{}^{si}(\mathbf{r}', \mathbf{r}_s). \tag{C3}$$

The fluorescent DPDW detected at position $\mathbf{r}$ and generated by the fluorophores at position $\underline{\mathbf{r}}'$ and the image fluorophores at position $\mathbf{r}'$ around volume element $\mathrm{d}\mathbf{r}'$ is

$$\delta\phi_{0f}{}^{si-z.b.c.}(\mathbf{r}, \mathbf{r}', \mathbf{r}_s) = \left[\frac{v S_f{}^{\mathrm{real}}(\mathbf{r}', \mathbf{r}_s)}{D_f} \frac{\exp(ik_f|\mathbf{r} - \mathbf{r}'|)}{4\pi|\mathbf{r} - \mathbf{r}'|} + \frac{v S_f{}^{\mathrm{img}}(\underline{\mathbf{r}}', \mathbf{r}_s)}{D_f} \frac{\exp(ik_f|\mathbf{r} - \underline{\mathbf{r}}'|)}{4\pi|\mathbf{r} - \underline{\mathbf{r}}'|} \right] \mathrm{d}\mathbf{r}'. \tag{C4}$$

The total fluorescent DPDW can be calculated by integrating Eq. (C4) over $z > 0$ half-space where the real fluorophores are distributed:

$$\begin{aligned}
&\phi_{0f}^{si-z.b.c.}(\mathbf{r}, \mathbf{r}_s) \\
&= \int_{z'>0} \left[\frac{v S_f^{\text{real}}(\mathbf{r}', \mathbf{r}_s)}{D_f} \frac{\exp(ik_f|\mathbf{r} - \mathbf{r}'|)}{4\pi|\mathbf{r} - \mathbf{r}'|} \right. \\
&\quad \left. + \frac{v S_f^{\text{img}}(\underline{\mathbf{r}}', \mathbf{r}_s)}{D_f} \frac{\exp(ik_f|\mathbf{r} - \underline{\mathbf{r}}'|)}{4\pi|\mathbf{r} - \underline{\mathbf{r}}'|} \right] d\mathbf{r}' \\
&= \frac{v^2 M_0}{D D_f} \frac{\sigma N_t}{1 - i\omega\tau} \int_{-\infty}^{\infty} dx' dy' \int_0^{\infty} dz' \\
&\quad \times \left[\frac{\exp(ik|\mathbf{r}' - \mathbf{r}_s|)}{4\pi|\mathbf{r}' - \mathbf{r}_s|} \frac{\exp(ik_f|\mathbf{r} - \mathbf{r}'|)}{4\pi|\mathbf{r} - \mathbf{r}'|} \right. \\
&\quad - \frac{\exp(ik|\mathbf{r}' - \underline{\mathbf{r}}_s|)}{4\pi|\mathbf{r}' - \underline{\mathbf{r}}_s|} \frac{\exp(ik_f|\mathbf{r} - \mathbf{r}'|)}{4\pi|\mathbf{r} - \mathbf{r}'|} \\
&\quad - \frac{\exp(ik|\mathbf{r}' - \mathbf{r}_s|)}{4\pi|\mathbf{r}' - \mathbf{r}_s|} \frac{\exp(ik_f|\mathbf{r} - \underline{\mathbf{r}}'|)}{4\pi|\mathbf{r} - \underline{\mathbf{r}}'|} \\
&\quad \left. + \frac{\exp(ik|\mathbf{r}' - \underline{\mathbf{r}}_s|)}{4\pi|\mathbf{r}' - \underline{\mathbf{r}}_s|} \frac{\exp(ik_f|\mathbf{r} - \underline{\mathbf{r}}'|)}{4\pi|\mathbf{r} - \underline{\mathbf{r}}'|} \right]. \qquad \text{(C5)}
\end{aligned}$$

When the variable is changed, e.g., $z' = -z'$, the fourth term in Eq. (C5) turns out to be

$$\begin{aligned}
&\frac{v^2 M_0}{D D_f} \frac{\sigma N_t}{1 - i\omega\tau} \int_{-\infty}^{\infty} dx' dy' \int_{-\infty}^{0} dz' \\
&\qquad \times \frac{\exp(ik|\mathbf{r}' - \mathbf{r}_s|)}{4\pi|\mathbf{r}' - \mathbf{r}_s|} \frac{\exp(ik_f|\mathbf{r} - \mathbf{r}'|)}{4\pi|\mathbf{r} - \mathbf{r}'|}.
\end{aligned}$$

We can combine the first and the fourth terms and obtain an integral similar to Eq. (5):

$$\begin{aligned}
(1) + (4) &= \frac{v^2 M_0}{D D_f} \frac{\sigma N_t}{1 - i\omega\tau} \int_{-\infty}^{\infty} d\mathbf{r}' \frac{\exp(ik|\mathbf{r}' - \mathbf{r}_s|)}{4\pi|\mathbf{r}' - \mathbf{r}_s|} \\
&\quad \times \frac{\exp(ik_f|\mathbf{r} - \mathbf{r}'|)}{4\pi|\mathbf{r} - \mathbf{r}'|} = \phi_{0f}(\mathbf{r}, \mathbf{r}_s). \qquad \text{(C6)}
\end{aligned}$$

The combination of the second and the third terms gives

$$\begin{aligned}
(2) + (3) &= -\frac{v^2 M_0}{D D_f} \frac{\sigma N_t}{1 - i\omega\tau} \int_{-\infty}^{\infty} d\mathbf{r}' \frac{\exp(ik|\mathbf{r}' - \underline{\mathbf{r}}_s|)}{4\pi|\mathbf{r}' - \underline{\mathbf{r}}_s|} \\
&\quad \times \frac{\exp(ik_f|\mathbf{r} - \mathbf{r}'|)}{4\pi|\mathbf{r} - \mathbf{r}'|} = -\phi_{0f}(\mathbf{r}, \underline{\mathbf{r}}_s). \qquad \text{(C7)}
\end{aligned}$$

Finally the fluorescent DPDW in a semi-infinite homogeneous system in which zero boundary conditions are used is

$$\phi_{0f}^{si-z.b.c.}(\mathbf{r}, \mathbf{r}_s) = \phi_{0f}(\mathbf{r}, \mathbf{r}_s) - \phi_{0f}(\mathbf{r}, \underline{\mathbf{r}}_s), \qquad \text{(C8)}$$

where $\phi_{0f}(\mathbf{r}, \mathbf{r}_s)$ and $\phi_{0f}(\mathbf{r}, \underline{\mathbf{r}}_s)$ are of the form of Eq. (6).

The authors are grateful for discussions with Michael Cohen and Eva Sevick-Muraca. A. G. Yodh acknowledges partial support from Mallinckrodt Medical, Inc., the National Science Foundation Presidential Young Investigator program, and the National Science Foundation under grant DMR93-06814. B. Chance acknowledges partial support from the National Institutes of Health under grants CA 50766 and CA 60182.

References and Notes

1. A. Yodh and B. Chance, "Spectroscopy and imaging with diffusing light," Phys. Today 31–36 (Mar. 1995) and references therein.
2. E. M. Sevick-Muraca and C. L. Burch, "Origin of phosphorescence signals reemitted from tissues," Opt. Lett. **19,** 1928–1930 (1994).
3. M. S. Patterson and B. W. Pogue, "Mathematical model for time-resolved and frequency-domain fluorescence spectroscopy in biological tissues," Appl. Opt. **33,** 1963–1974 (1994).
4. A. Knüttel, J. M. Schmitt, R. Barnes, and J. R. Knutson, "Acousto-optic scanning and interfering photon density waves for precise localization of an absorbing (or fluorescent) body in a turbid medium," Rev. Sci. Instrum. **64,** 638–644 (1993).
5. D. A. Boas, M. A. O'Leary, B. Chance, and A. G. Yodh, "Scattering and wavelength transduction of diffuse photon density waves," Phys. Res. E **47,** R2999–R3002 (1993).
6. M. A. O'Leary, D. A. Boas, B. Chance, and A. G. Yodh, "Reradiation and imaging of diffuse photon density waves using fluorescent inhomogeneities," J. Luminesc. **60-1,** 281–286 (1994).
7. X. D. Li, B. Beauvoit, R. White, S. Nioka, B. Chance, and A. G. Yodh, "Tumor localization using fluorescence of indocyanine green (ICG) in rat models," in *Optical Tomography, Photon Migration, and Spectroscopy of Tissue and Model Media: Theory, Human Studies, and Instrumentation,* B. Chance and R. R. Alfano, eds., Proc. SPIE **2389,** 789–797 (1995).
8. J. Wu, Y. Wang, L. Perelman, I. Itzkan, R. R. Dasari, and M. S. Feld, "Time-resolved multichannel imaging of fluorescent objects embedded in turbid media," Opt. Lett. **20,** 489–491 (1995).
9. S. B. Bambot, J. R. Lakowicz, and G. Rao, "Potential applications of lifetime-based, phase-modulation fluorimetry in bioprocess and clinical monitoring," Trends Biotechnol. **13,** 106–115 (1995).
10. W. L. Rumsey, J. M. Vanderkooi, and D. F. Wilson, "Imaging of phosphorescence: a novel method for measuring oxygen distribution in perfused tissue," Science **241,** 1649–1651 (1988).
11. H. Szmacinski and J. R. Lakowicz, "Optical measurements of pH using fluorescence lifetimes and phase-modulation fluorometry," Anal. Chem. **65,** 1668–1674 (1993).
12. J. R. Lakowicz, H. Szmacinski, K. Nowaczyk, and M. L. Johnson, "Fluorescence lifetime imaging of calcium using Quin-2," Cell Calcium **13,** 131–147 (1992).
13. J. Folkman, "Introduction: angiogenesis and cancer," Semin. Cancer Biol. **3,** 65–71 (1992).
14. P. W. Vaupel, S. Frinak, and H. I. Bicher, "Heterogeneous oxygen partial pressure and pH distribution in C3H mouse mammary adenocarcinoma," Cancer Res. **41,** 2008–2013 (1981).
15. C. L. Hutchinson, T. L. Troy, and E. M. Sevick-Muraca, "Fluorescence-lifetime spectroscopy and imaging in random media," in *Optical Tomography, Photon Migration, and Spectroscopy of Tissue and Model Media: Theory, Human Studies, and Instrumentation,* B. Chance and R. R. Alfano, eds. Proc. SPIE **2389,** 274–283 (1995).

16. C. L. Hutchinson, J. R. Lakowicz, and E. M. Sevick-Muraca, "Fluorescence lifetime-based sensing in tissues: a computational study," Biophys. J. **68,** 1574–1582 (1995).
17. J. Wu, M. S. Feld, and R. P. Rava, "Analytical model for extracting intrinsic fluorescence in turbid media," Appl. Opt. **32,** 3585–3595 (1993).
18. We are aware that faster finite difference methods exist. However, none of these methods is expected to be faster than calculations of the analytic solutions.
19. M. S. Patterson, B. Chance, and B. C. Wilson, "Time-resolved reflectance and transmittance for the noninvasive measurement of tissue optical properties," Appl. Opt. **28,** 2331–2335 (1989).
20. J. B. Fishkin and E. Gratton, "Propagation of photon density waves in strongly scattering media containing an absorbing semi-infinite plane bounded by a straight edge," J. Opt. Soc. Am. A **10,** 127–140 (1993).
21. B. J. Tromberg, S. Madsen, C. Chapman, L. O. Svaasand, and R. C. Haskell, "Frequency-domain photon migration in turbid media," in *Advances in Optical Imaging and Photon Migration,* Vol. 21 of OSA Proceedings (Optical Society of America, Washington, D.C., 1994), pp. 93–95.
22. D. A. Boas, M. A. O'Leary, B. Chance, and A. G. Yodh, "Scattering of diffuse photon density waves by spherical inhomogeneities within turbid media: analytic solutions and applications," Proc. Natl. Acad. Sci. USA **91,** 4887–4891 (1994).
23. R. C. Haskell, L. O. Svaasand, T. T. Tsay, T. C. Feng, M. S. McAdams, and B. J. Tromberg, "Boundary conditions for the diffusion equation in radiative transfer," J. Opt. Soc. Am. A **11,** 2727–2741 (1994).
24. R. Aronson, "Boundary conditions for diffusion of light," J. Opt. Soc. Am. A **12,** 2532–2539 (1995).
25. S. J. Madsen, M. S. Patterson, B. C. Wilson, S. M. Jaywant, and A. Othonos, "Numerical modeling and experimental studies of light pulse propagation in inhomogeneous random media," in *Photon Migration and Imaging in Random Media and Tissues,* B. Chance and R. R. Alfano, eds., Proc. SPIE **1888,** 90–102 (1993).
26. P. W. Milonni and J. H. Eberly, *Lasers* (Wiley, New York, 1988), pp. 218–222.
27. J. R. Lakowicz, *Principles of Fluorescence Spectroscopy* (Plenum, New York, 1983), pp. 258–266.
28. G. Valduga, E. Reddi, G. Jori, R. Cubeddu, P. Taroni, and G. Valentini, "Steady state and time-resolved spectroscopic studies on zinc(II) phthalocynine in liposomes," J. Photochem. Photobiol. B: Biol. **16,** 331–340 (1992); R. Cubeddu, G. Canti, P. Taroni, and G. Valentini, "Time-gated fluorescence imaging for the diagnosis of tumors in a murine model," Photochem. Photobiol. **57,** 480–485 (1993).
29. M. A. O'Leary, D. A. Boas, X. D. Li, B. Chance, and A. G. Yodh, "Fluorescence lifetime imaging in turbid media," Opt. Lett. **21,** 158–160 (1996).